applied sciences

MDPI

Article

AtTPR10 Containing Multiple ANK and TPR Domains Exhibits Chaperone Activity and Heat-Shock Dependent Structural Switching

Seol Ki Paeng, Chang Ho Kang, Yong Hun Chi, Ho Byoung Chae, Eun Seon Lee, Joung Hun Park, Seong Dong Wi, Su Bin Bae, Kieu Anh Thi Phan and Sang Yeol Lee *

Division of Applied Life Science (BK21+) and Plant Molecular Biotechnology Research Center, Gyeongsang National University, Jinju 52828, Korea; skpaeng@gmail.com (S.K.P.); jacobgnu69@gnu.ac.kr (C.H.K.); gandhi37@gnu.ac.kr (Y.H.C.); truedaisy@hanmail.net (H.B.C.); dmstjsl88@hanmail.net (E.S.L.); jazzc@nate.com (J.H.P.); wsd3377@gmail.com (S.D.W.); dnflwlq7760@naver.com (S.B.B.); phanthikieuanh95@gmail.com (K.A.T.P.)

* Correspondence: sylee@gnu.ac.kr; Tel.: +82-55-772-1351

Received: 13 January 2020; Accepted: 10 February 2020; Published: 13 February 2020

Abstract: Among the several tetratricopeptide (TPR) repeat-containing proteins encoded by the *Arabidopsis thaliana* genome, AtTPR10 exhibits an atypical structure with three TPR domain repeats at the C-terminus in addition to seven ankyrin (ANK) domain repeats at the N-terminus. However, the function of AtTPR10 remains elusive. Here, we investigated the biochemical function of AtTPR10. Bioinformatic analysis revealed that *AtTPR10* expression is highly enhanced by heat shock compared with the other abiotic stresses, suggesting that AtTPR10 functions as a molecular chaperone to protect intracellular proteins from thermal stresses. Under the heat shock treatment, the chaperone activity of AtTPR10 increased significantly; this was accompanied by a structural switch from the low molecular weight (LMW) protein to a high molecular weight (HMW) complex. Analysis of two truncated fragments of AtTPR10 containing the TPR and ANK repeats showed that each domain exhibits a similar range of chaperone activity (approximately one-third of that of the native protein), suggesting that each domain cooperatively regulates the chaperone function of AtTPR10. Additionally, both truncated fragments of AtTPR10 underwent structural reconfiguration to form heat shock-dependent HMW complexes. Our results clearly demonstrate that AtTPR10 functions as a molecular chaperone in plants to protect intracellular targets from heat shock stress.

Keywords: ankyrin; tetratricopeptide; heat shock tolerant; holdase chaperone; structural switching

1. Introduction

Terrestrial plants face diverse abiotic and biotic stresses during their life cycles. To cope with these environmental stresses, plants employ various important defense-associated proteins, such as pathogenesis-related (PR) proteins (chitinase, glucanase, thaumatin, defensin, and thionin), stress-resistant peptides, and highly efficient defense signaling systems. Among the defense-related proteins, tetratricopeptide (TPR) repeat proteins, which mediate protein–protein interactions, assemble as multiprotein complexes to defend against external stresses [1–3]. The *Arabidopsis thaliana* genome encodes more than 16 TPR-containing proteins. Previously, TPR motifs were detected in the FKBP52 protein, which facilitates the folding of target proteins with the help of heat shock protein 90 (HSP90) [4], and in cyclophilin 40 (CyP40), a cyclosporine A-binding immunophilin that supports protein stability and refolding of protein aggregates through the action of its hydrophobic regions [5]. In addition, CHIP, a ubiquitin E3-ligase protein containing three TPR repeats and a U-box domain, protects membrane channel proteins and degrades damaged proteins under extreme temperature

conditions [6,7]. In *Arabidopsis*, TPR motif-containing proteins have been reported to function in the regulation of plant growth and development and hormone signaling [8]. Thus, the TPR-repeat thioredoxin (Trx)-like 1 (TTL1) protein affects abscisic acid (ABA) sensitivity and osmotic stress responses in plants [9]. Ectopic expression of the *spindly* (*SPY*) gene showed that SPY functions as a negative regulator of gibberellin (GA) response, affecting hypocotyl elongation and flowering time in plants [10]. In rice (*Oryza sativa* L.), the Trx-like protein OsTDX, which contains three N-terminal TPR motifs and a C-terminal Trx domain, exhibits defense activity against various fungal pathogens [11]. Moreover, OsTPR1 participates in the immune response by disturbing the interaction between chitin and MoChia1, a suppressor of chitin-triggered plant immunity [12].

In contrast to other types of *Arabidopsis* TPRs, AtTPR10 contains seven N-terminal repeats of the ankyrin (ANK) domain and three C-terminal repeats of the TPR domain. Similar to the TPR motifs, the ANK repeat domains mediate protein–protein interaction in diverse organisms including eukaryotes, prokaryotes, and some viruses [13,14]. The domains also contain several conserved hydrophobic residues necessary for maintaining their secondary and tertiary structures [15–17]. Genomic analyses revealed a total of 509 ANK repeats in more than 100 proteins in *Arabidopsis* with structurally similar characteristics. The ANK repeat-containing plant proteins regulate the cell cycle, mitochondrial enzyme activity, ion transport, and signal transduction [13].

These data suggest that the two domains play diverse physiological roles in plants by associating with different partner proteins. Although the AtTPR10 protein consists of two highly important domains (TPR and ANK) in a single polypeptide structure, its molecular function remains unknown. Here, we performed bioinformatics analysis of *AtTPR10* gene expression and investigated the biochemical characteristics of the AtTPR10 protein. Our results show that AtTPR10 functions as a molecular chaperone to protect plants from diverse abiotic stresses that can be used for the development of stress-tolerant crops.

2. Materials and Methods

2.1. Plasmid Construction and Recombinant Protein Purification

Sequences of the full-length *AtTPR10* gene, ankyrin domain (*ANK-D*), and TPR domain (*TPR-D*) were amplified from the *Arabidopsis* cDNA library by PCR using the primer pairs AtTPR10 forward (F)/AtTPR10 reverse (R) (5′-GGATCCATGGCTCCTGATGC-TTCTACT-3′/5′-GTCGACTTATGA-TTTGGCCTTAACCTC-3′), ANK-D_F/ANK-D_R (5′-GGATCCATGAACAAACGTGGAGCGCTT-CACT-3′/5′-GTCGACTTAAGTT TCTGGTTTTGTTGTCAATGGG-3′), and TPR-D_F/TPR-D_R (5′-GGATCCATGGCCGCAGAAGCAA AAGCCA-3′/5′-GTCGACTTAGCTTTCAGGGCTAAGCAAT-ACTCC-3′), respectively. The PCR products were cloned into the *pGEM-T*^{easy} vector (Promega Co., Madison, USA), and the resulting *pGEM-T*^{easy}*-AtTPR10*, *-ANK-D*, and *-TPR-D* constructs were sequenced. Then, these plasmids were digested with *Bam*HI and *Sal*I, and cloned into the *pGEX-2T* expression vector (New England Biolab, Ipswich, MA, USA) to generate fusions with the *glutathione S-transferase* (*GST*) gene, and the resulting DNA constructs were used for protein expression in *Escherichia coli* BL21 (DE3) cells. The transformed bacteria were grown in Luria broth (LB) containing 50 μg/μL ampicillin at 37 °C until the optical density at 600 nm absorbance ($O.D._{600}$) approached 0.7. Then, expression of the recombinant GST fusion proteins was induced by the addition of 0.4 mM isopropyl β-D-1-thiogalactopyranoside (IPTG), and the cells were cultured for another 5 h. The cells were then harvested by centrifugation at 6000× *g* for 5 min, and the pellet was resuspended in 1X phosphate-buffered saline (PBS; 140 mM NaCl, 2.7 mM KCl, 10 mM Na_2HPO_4, and 1.8 mM KH_2PO_4 [pH 7.6]). The GST-AtTPR10, GST-ANK-D, and GSR-TPR-D fusion proteins were purified from the cells using GST agarose resin, and the eluted GST-tagged proteins were cleavaged by thrombin. The mature proteins were then analyzed by dialysis using 50 mM HEPES-KOH (pH 8.0). Each protein was further purified using a TSK G4000SW_{XL} high performance liquid chromatography (HPLC) column (30 cm × 7.8 mM), as described previously [18,19].

2.2. Determination of Holdase Chaperone Activity

Holdase chaperone activity was measured using malate dehydrogenase (MDH; Sigma-Aldrich) and citrate synthase (CS) as substrates [20,21]. MDH and CS were incubated with AtTPR10, ANK-D, and TPR-D in 50 mM HEPES-KOH (pH 8.0) at 43 °C for 15 min, and the heat-induced thermal aggregation of both substrates was monitored using a DU800 spectrophotometer (Beckman, Brea, CA, USA) equipped with a thermostatic cell holder preheated to 43 °C, as described previously [22].

2.3. Size Exclusion Chromatography (SEC)

HPLC (Dionex, Sunnyvale, CA, USA) was carried out at 23 °C on a Superdex 200 HR 10/30 column equilibrated with 50 mM HEPES-KOH (pH 8.0) containing 100 mM NaCl. Proteins were eluted using the same buffer at a flow rate of 0.5 mL/min, as described previously [23]. The fractionated protein peaks (A_{280}) were isolated and concentrated at 4 °C using a Centricon YM-10 (Millipore, Billerica, MA, USA).

2.4. Measurement of Bis-ANS Fluorescence

A mixture of AtTPR10, ANK-D, and TPR-D (20 µg/mL each) in 50 mM HEPES (pH 8.0) was added to 10 µM 4,4′-*bis*(phenylamino)-[1,1′-binaphthalene]-5,5′-disulfonic acid dipotassium salt (bis-ANS), and the resulting mixture was incubated at 23 °C for 30 min. Excess bis-ANS was removed by dialysis using the sample buffer, and its fluorescence intensity was measured using a SFM25 spectrofluorometer (Kontron, Instruments SpA, Milan, Italy), as described previously [22].

2.5. Abiotic Stress Treatments and AtTPR10 Expression Analysis

Two-week-old seedlings of *Arabidopsis thaliana* ecotype Columbia (Col-0; wild-type [WT]) were grown in Murashige and Skoog (MS) medium containing 3% sucrose. To perform the heat shock treatment, temperature was increased from 23 °C to 37 °C or 45 °C and then held constant for 3 h [24]. To conduct the cold treatment, the temperature of soil-grown plants was decreased from 23 °C to 4 °C and then held constant for 48 h [25]. To induce salt stress, soil-grown plants were incubated in a solution containing 250 mM NaCl for 48 h [26]. To induce drought stress, plants grown in MS medium for seven days were transferred to soil and grown for one week with sufficient watering; then, watering was withheld for two days [27,28].

To determine *AtTPR10* expression under various abiotic stresses, samples were collected at the indicated time points, immediately frozen in liquid nitrogen, and used for RNA extraction and subsequent analysis. Real-time polymerase chain reaction (RT-PCR) was performed to amplify *AtTPR10* using gene-specific primers (AtTPR10 RT_F, 5′-CTGTGGAAGTCTTGTTAGAAC-ACAATGCC-3′; AtTPR10 RT_R, 5′-GGTATGATCCGTTGGGTCAAAATCAATT-3′). Tubulin, which was used as the loading control, was amplified using the following primers: Tubulin F (5′-CTCAAGAGGTTCTCAGCAGTA-3′) and Tubulin R (5′-TCACCTTCTTCATCCGCAGTT-3′).

2.6. Heat Stability Analysis of AtTPR10

To determine the heat stability of AtTPR10, 1 µg each of the recombinant MDH and AtTPR10 proteins was incubated at 23 °C, 50 °C, and 60 °C for 15 min. Proteins were then centrifuged at 13,000× *g* for 20 min. The supernatant and pellet fractions were analyzed by sodium dodecyl sulfate polyacrylamide gel electrophoresis (SDS-PAGE) using a 12% gel, followed by Coomassie brilliant blue staining. The solubility ratio of each protein was calculated by dividing the band density of the supernatant fraction with that of the pellet fraction by densitometer.

2.7. Validation of AtTPR10 Expression in Response to Abiotic Stresses

Expression patterns of *AtTPR10* under various abiotic stresses were analyzed using the *Arabidopsis* eFP Browser v2.0 (http://bar.utoronto.ca/efp2/Arabidopsis/Arabidopsis_eFPBro-wser2.html).

This browser contained expression data from *Arabidopsis* shoots subjected to different abiotic stresses for 12 h.

2.8. Native Gel Electrophoresis

Native PAGE gel was used for separation of proteins in their native conformation. Heat shock treated protein samples were isolated from insoluble proteins by centrifugation at 13,000× *g* for 15 min; the supernatants were obtained to new e-tubes, and the supernatant fraction was measured by Bradford's method. Protein samples were mixed with nonreducing–nondenaturing sample buffer (125 mM Tris-HCl, pH 6.8, 20% glycerol, and 0.1% Bromophenol blue). Equal amounts of protein samples were subjected to 10% native PAGE gel [23,29]. After finishing the native gel electrophoresis, their structural properties were analyzed by silver staining method.

3. Results

3.1. Bioinformatic Analysis of AtTPR10 Function

The *Arabidopsis* genome encodes more than 21 AtTPR proteins. These proteins are classified on the basis of their molecular structure and the presence or absence of the TPR domain and/or other motifs (Figure 1). Among the proteins, *AtTPR10* (At3g04710) showed a peculiar structure with both TPR and ANK domains in a single polypeptide that is possibly involved in protein–protein interactions, protein assembly, and signal transduction [1,30–33]. The AtTPR10 protein is a 456 amino acid (aa) protein with seven N-terminal ANK domains (54–280 aa) and three C-terminal TPR domains (328–429 aa) (Figure 2).

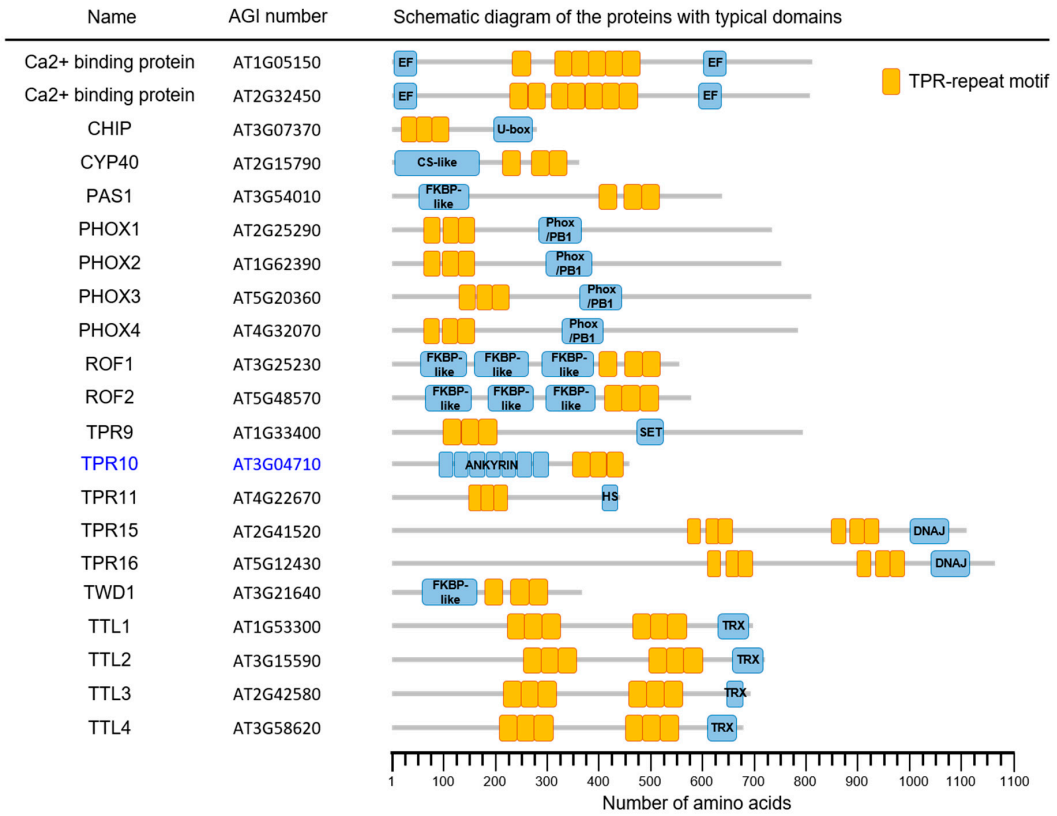

Figure 1. Schematic representation of the tetratricopeptide (TPR) repeat-containing proteins encoded by the *Arabidopsis* genome. These proteins contain several copies of the TPR domain (orange boxes), along with other functional domains (blue boxes). Among them, TPR10 domains selected in this study are indicated as blue characters. The scale at the bottom indicates the number of amino acid residues in these proteins.

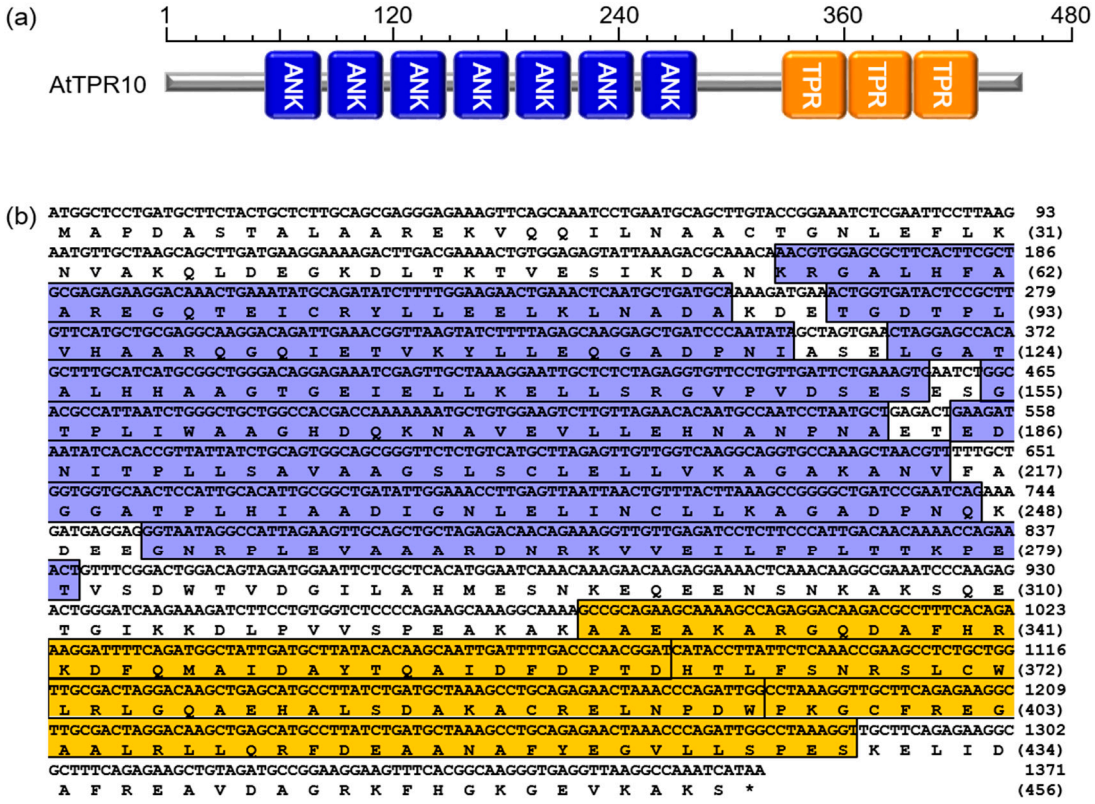

Figure 2. Typical features of *AtTPR10*. (**a**) Schematic representation of AtTPR10 structure containing seven N-terminal ankyrin (ANK) repeats and three C-terminal TPR repeats. (**b**) Nucleotide and amino acid sequences of AtTPR10. The ANK repeats are indicated in blue, while the TPR domains are indicated in orange. Asterisk (*) indicates the stop codon.

To determine the function of AtTPR10 in plants, we investigated its mRNA expression under diverse abiotic stresses using microarray data (*Arabidopsis* eFP Browser v2.0; http://bar.u-toronto.ca/efp2/Arabidopsis/Arabidopsis_eFPBrowser2.html). Results showed that the transcript level of *AtTPR10* was specifically upregulated by heat stress (Figure 3a) but not by the other abiotic stresses, such as cold, salt, and drought. This prediction was confirmed by real-time polymerase chain reaction (RT-PCR), which revealed the upregulation of *AtTPR10* transcripts by heat stress treatment at 37 °C and 45 °C (Figure 3b). Additionally, *AtTPR10* expression was gradually induced by heat stress (37 °C) within 1 h after treatment (Figure 3c), suggesting that the functional role of the protein might be involved in heat resistance in plants. By contrast, *AtTPR10* was non-responsive to other abiotic stresses, including cold, salt, and drought (Figure 3d).

In addition to *AtTPR10* expression analysis under heat shock treatment, we also examined the heat stability of the AtTRP10 protein. Recombinant AtTPR10 purified from *E. coli* was treated with high temperatures (50 °C, and 60 °C) for 15 min and then centrifuged at 13,000× *g* for 20 min. The supernatant and pellet fractions were analyzed by SDS-PAGE, followed by Coomassie brilliant blue staining. Most of the AtTPR10 protein showed high stability at all temperatures tested, unlike the malate dehydrogenase MDH used as a control (Figure 4). At 60 °C, more than 95% of the AtTPR10 protein was present in the supernatant fraction; by contrast, less than 2% of the MDH remained in the supernatant, while most of the MDH was precipitated by heat-induced aggregation (Figure 4a,b). These results strongly suggest that AtTPR10 is highly thermo-stable and its function possibly includes heat shock resistance in plant cells.

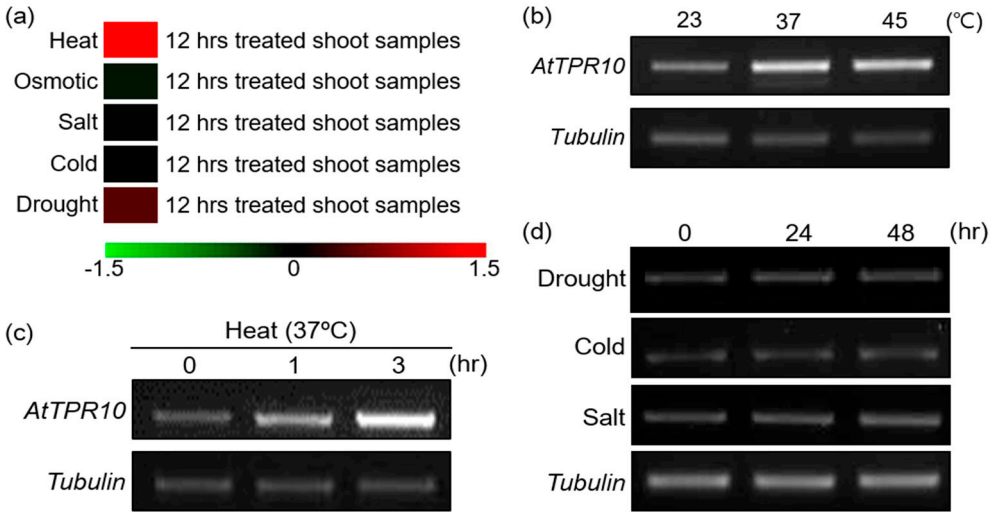

Figure 3. Expression analysis of *AtTPR10* under diverse abiotic stresses via bioinformatics database searches. (**a**) Effect of AtTPR10 expression in *Arabidopsis* by the treatment of abiotic stress examined in the database of *Arabidopsis* eFP Browser v2.0 (http://bar.utoronto.ca/efp2/Arabidopsis/Ara-bidopsis_eFPBrowser2.html). (**b**)–(**d**) RT-PCR analysis of *AtTPR10* expression in two-week-old WT (Col-0) *Arabidopsis* seedlings treated with heat stress (**b**) and (**c**) and other abiotic stresses (**d**). Plants were grown in MS medium containing 3% sucrose, and temperature was changed from 23 °C to 37 °C or 45 °C for 3 h (heat shock treatment) or to 4 °C for 48 h (cold treatment). To induce salt stress, plants were treated with 250 mM NaCl for 48 h. To perform the drought stress treatment, WT seedlings grown in MS medium for seven days were transferred to soil and grown for one week with sufficient watering. Then, watering was withheld for two days to induce drought stress. *Tubulin* was used as the loading control in all RT-PCR experiments.

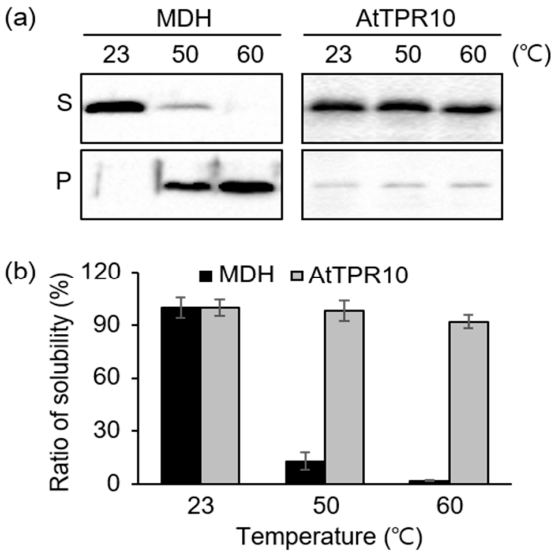

Figure 4. Stability of AtTPR10 under heat stress. (**a**) Heat stability analysis of AtTPR10 and malate dehydrogenase (MDH; control). Approximately 1 μg each of AtTPR10 and MDH was incubated at 23 °C, 50 °C, and 60 °C for 15 min and then centrifuged at 13,000× *g* for 20 min. The supernatant (S) and pellet (P) fractions were analyzed by SDS-PAGE, followed by Coomassie brilliant blue staining. (**b**) Solubility ratio of AtTPR10 and MDH at different temperatures. Protein bands shown in (**a**) were scanned with a densitometer. Solubility ratio was determined by dividing the supernatant density with the pellet density for each sample. The representative results are means of at least three independent experiments.

3.2. Heat Shock-Dependent Structural Switching of AtTPR10

Next, we examined the structure of AtTPR10 under heat stress by native gel electrophoresis and size exclusion chromatography (SEC) using HPLC. Heat-shock treated recombinant AtTPR10 protein samples produced a single band on SDS-PAGE gel (Figure 5a, bottom panel). While the AtTPR10 showed a single protein band in SDS-PAGE gel, it showed multiple bands in the native gel at 23 °C, indicating that the AtTPR10 protein exists as different structural isoforms including monomers, oligomers, and high molecular weight (HMW) complexes (Figure 5a, upper panel, lane #1). However, heat treatment induced significant structural shifts from low MW (LMW) protein species to HMW complexes. Thus, upon incubation of the protein at 60 °C for 30 min, most of the LMW species formed HMW complexes (Figure 5a, upper panel, lane #3). This structural shift was confirmed by SEC. Under normal conditions (23 °C), AtTPR10 displayed several discrete peaks representing monomers, oligomers and HMW complexes; however, under heat stress, most of the peaks representing LMW species in the SEC chromatogram disappeared, and the peak representing HMW complexes increased in size, indicating that the LMW species formed HMW complexes at high temperatures (Figure 5b). The heat shock-dependent formation of HMW complexes suggests that the AtTPR10 protein interacts with itself and forms higher MW complexes mainly by hydrophobic interaction. Therefore, we examined changes in the surface hydrophobicity of AtTPR10 in response to high temperature by incubating the protein with bis-ANS (probe) (Figure 5c). Bis-ANS binds to hydrophobic patches of proteins and emits fluorescence at 470 nm [22]. The fluorescence intensity of the bis-ANS peak (observed at 480 nm) was significantly higher at 60 °C than at 23 °C, indicating that several hydrophobic patches of AtTPR10 are exposed at high temperatures, enabling the formation of supra-structures. This confirms the propensity of AtTPR10 to form HMW complexes at high temperatures.

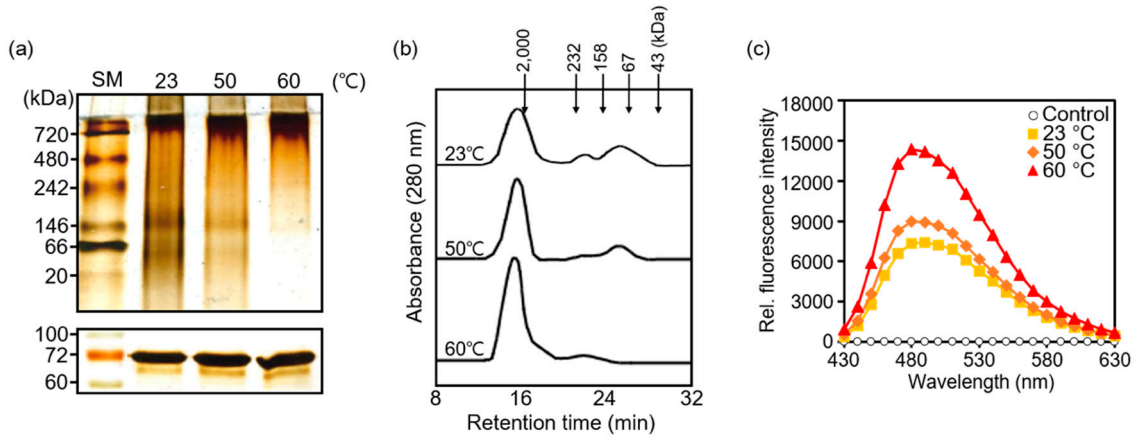

Figure 5. Heat shock-dependent changes in AtTPR10 structure and hydrophobicity. (**a**) Structural changes in AtTPR10 in response to the heat shock treatment. AtTPR10 was incubated at 23 °C, 50 °C, and 60 °C for 30 min, centrifuged at 13,000× *g* for 15 min, and analyzed by 10% native PAGE gel and silver staining. SM represents the size marker. (**b**) Size exclusion chromatography (SEC) analysis of AtTPR10 by HPLC. Recombinant purified AtTPR10 was heat-treated, as described in (**a**), and 2 mg of each protein sample was separated by SEC, based on the MW. (**c**) Heat-shock dependent changes in the surface hydrophobicity of AtTPR10. Recombinant AtTPR10 protein (20 µg) was incubated with 10 µM bis-ANS at 23 °C (■), 50 °C (◆), and 60 °C (▲) for 20 min. Incubation of 10 µM bis-ANS with no AtTPR10 protein served as a control (○). The fluorescence intensity of bis-ANS was measured at an excitation wavelength of 390 nm and emission spectra of 430–630 nm.

3.3. AtTPR10 Acts as a Molecular Chaperone

Since heat stability and temperature-dependent structural shifts are representative characteristics of molecular chaperones [5–7,34,35], we investigated whether AtTPR10 acts as a molecular chaperone. The chaperone activity of AtTPR10 was measured by its ability to protect target substrate proteins,

such as MDH and CS, from denaturation under heat stress (Figure 6). During the heat treatment, formation of insoluble aggregates of denatured CS and MDH was measured by monitoring the degree of light scattering using a temperature-controlled spectrophotometer at 340 nm. In this experiment, 2-Cys Prx (a strong molecular chaperone) and GST were used as positive and negative controls, respectively [23,36].

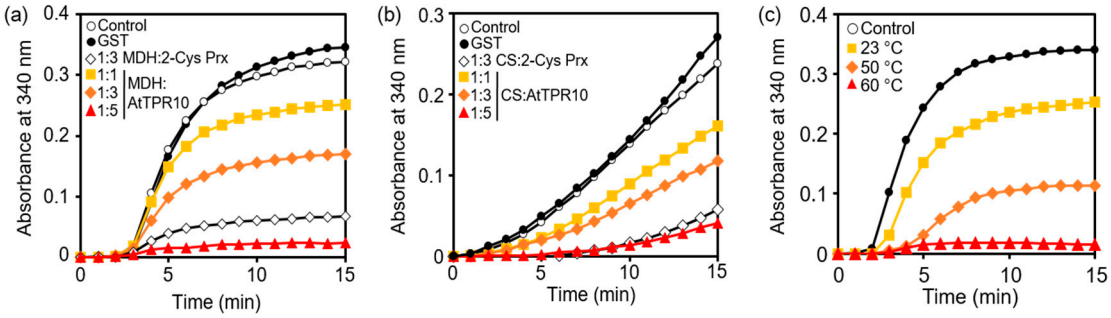

Figure 6. Chaperone activity analysis and heat shock-dependent activity regulation of AtTPR10. (**a**) and (**b**) Analysis of the chaperone function of AtTPR10 using MDH (**a**) and citrate synthase (CS) (**b**) as substrates. Thermal aggregation of MDH and CS was monitored at 340 nm after a 15 min incubation with AtTPR10. In (**a**), 1.5 μM MDH was incubated at 43 °C, either alone (○; control) or with 7.5 μM GST (●), 4.5 μM 2-Cys Prx (◇), and 1.5 μM (■), 4.5 μM (◆), and 7.5 μM (▲) AtTPR10 in 50 mM HEPES (pH 7.0). In (**b**), 1.2 μM CS was incubated at 43 °C, either alone (○; control) or with 6 μM GST (●), 3.6 μM 2-Cys Prx (◇) and 1.2 μM (■), 3.6 μM (◆), and 6 μM (▲) AtTPR10 in 50 mM HEPES (pH 7.0). (**c**) Heat-shock dependent chaperone activity of AtTPR10. In this experiment, 1.5 μM MDH was incubated either alone (○; control) or with 3 μM AtTPR10 at 23 °C (■), 50 °C (◆r), and 60 °C (▲) for 15 min.

Both AtTPR10 and 2-Cys Prx effectively prevented the thermal denaturation of the target substrate (MDH) at 43 °C; however, GST showed no protective function with either substrate (MDH or CS) under the same conditions (Figure 6a,b). When the molar ratio of AtTPR10 to MDH was increased, the protective function of AtTPR10 increased significantly; at the AtTPR10:MDH molar ratio of 5:1, nearly perfect protection was achieved within 15 min of the heat treatment. This result clearly demonstrates that AtTPR10 functions as a molecular chaperone under heat stress. Additionally, the chaperone activity of AtTPR10 was critically enhanced by a 15 min heat shock treatment at 60 °C (Figure 6c). These results strongly suggest that AtTPR10 performs the biochemical function of a molecular chaperone to protect intracellular molecules from heat stress.

3.4. ANK and TPR Domains Work Together as a Molecular Chaperone

Because AtTPR10 showed molecular chaperone activity (Figure 6) and contains two domains, ANK and TPR (Figure 2), which are reported to be involved in protein–protein interactions and intracellular protein complex assembly [4,5,7,21,34], we analyzed the contribution of each domain to the chaperone function of AtTPR10. To do the experiment, two truncated versions of the AtTPR10 protein, ANK-D (1–300 aa) and TPR-D (300–456 aa), were constructed (Figure 7a). These truncated recombinant proteins were expressed in *E. coli*, homogeneously purified, and used for biochemical analysis (Figure 7b). Chaperone activity of the truncated proteins was measured using MDH and CS as substrates at a truncated protein:substrate molar ratio of 1:5. Both domains exhibited a similar level of chaperone activity (Figure 7c), but each truncated protein showed approximately 30%–40% lower chaperone activity than the native AtTPR10. This suggests that each domain contributes to the chaperone function of AtTPR10 in a synergistic manner. To investigate the structural changes in the truncated proteins, we analyzed the hydrophobicity of these proteins by incubation with bis-ANS. Consistent with the result of chaperone activity, the hydrophobicity of AtTPR10 was considerably higher than that of each truncated protein (Figure 7d).

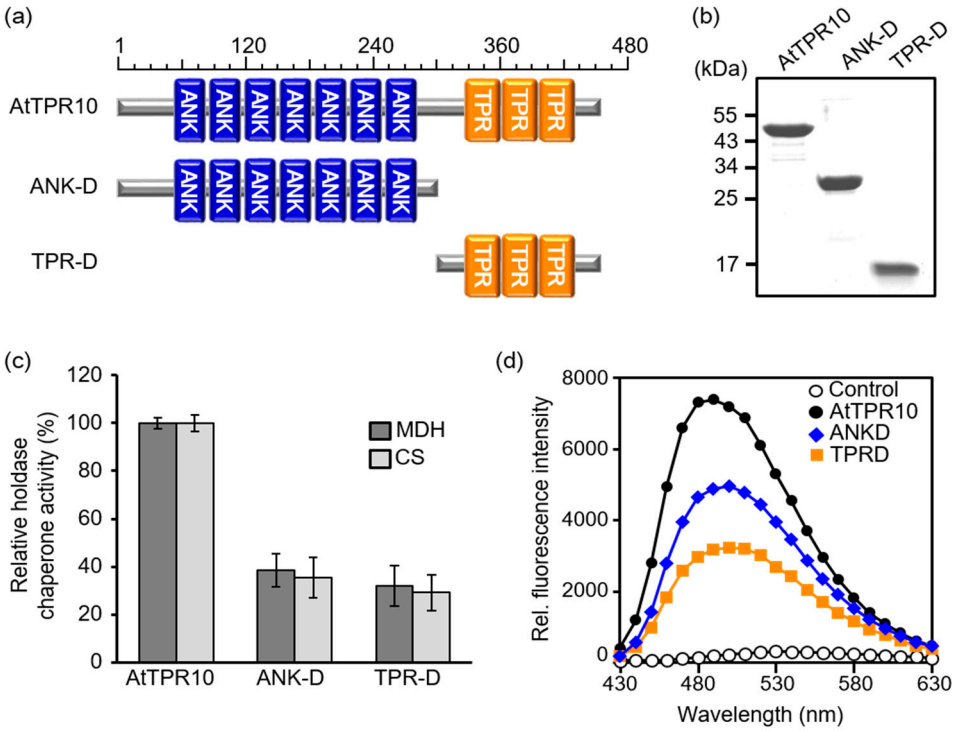

Figure 7. Comparison of the chaperone activity and hydrophobicity of AtTPR10, ANK-D, and TPR-D. (**a**) Schematic representation of AtTPR10 and its truncated variants. (**b**) Purification of homogeneous recombinant proteins analyzed by SDS-PAGE gel. Each protein was separated on a 12% denaturing gel by SDS-PAGE and visualized by Coomassie Brilliant Blue staining. Numbers indicate the molecular weight standards in kDa. (**c**) Relative chaperone activity of AtTPR10 and its truncated forms. The data presented are the averages of at least three independent measurements. (**d**) Comparison of the hydrophobicity of AtTPR10, ANK-D, and TPR-D, following incubation with bis-ANS at 23 °C. Fluorescence of bis-ANS was measured at an excitation wavelength of 390 nm and emission spectra of 430–630 nm. Only bis-ANS treatment was used as control.

Furthermore, because the chaperone activity of AtTPR10 increased upon heat shock treatment (Figure 6c), we investigated changes in the chaperone activity and hydrophobicity of the truncated mutants under different temperatures (Figure 8). Similar to AtTPR10 (Figure 6c), chaperone activity of ANK-D and TPR-D increased significantly upon increasing the temperature from 23 °C to 60 °C (Figure 8a). Additionally, exposure of the hydrophobic surfaces of the truncated proteins at different temperatures was verified by incubation with bis-ANS (Figure 8b,c).

In contrast to the hydrophobicity of proteins under normal temperature (23 °C), the proportion of hydrophobic patches on the surface was greatly increased to allow the binding of denatured substrates under heat stress. In addition, chaperone activities of both truncated proteins were greatly enhanced by the heat shock treatment, suggesting that the structure of these proteins was transformed by thermal exposure. Because AtTPR10 polymerized and formed HMW complexes in response to high temperature (Figure 5a,b), we examined the heat stress-induced structural shift in the two truncated proteins by native gel electrophoresis and SEC. The results of native gel electrophoresis showed that the MW of both ANK-D and TPR-D increased significantly under high temperatures (Figure 9a,c), similar to ATPR10. These structural shifts were confirmed by the HPLC–SEC experiment (Figure 9b,d). Upon exposure to 60 °C for 30 min, both ANK-D and TPR-D were predominantly present as HMW complexes, indicating that the monomeric and oligomeric forms of each truncated protein interacted to form HMW complexes.

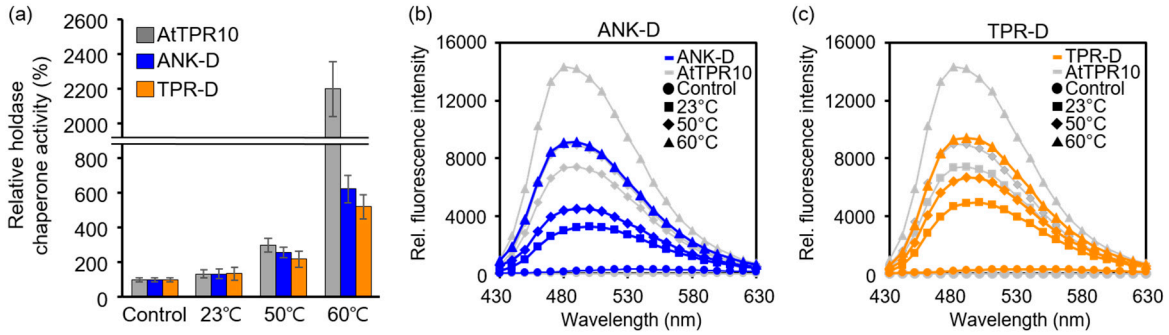

Figure 8. Comparison of the chaperone activity and hydrophobicity of AtTPR10, ANK-D, and TPR-D at different temperatures. (**a**) Relative chaperone activity of AtTPR10, ANK-D, and TPR-D at 23 °C, 50 °C, and 60 °C. (**b**) and (**c**) Hydrophobicity analysis of ANK-D (**b**) and TPR-D (**c**), along with that of AtTPR10, upon incubation with bis-ANS at 23 °C, 50 °C, and 60 °C for 30 min. The fluorescence of bis-ANS was measured using a fluorometer, with excitation at 390 nm and emission at 430–630 nm. The representative results are means of at least three independent experiments.

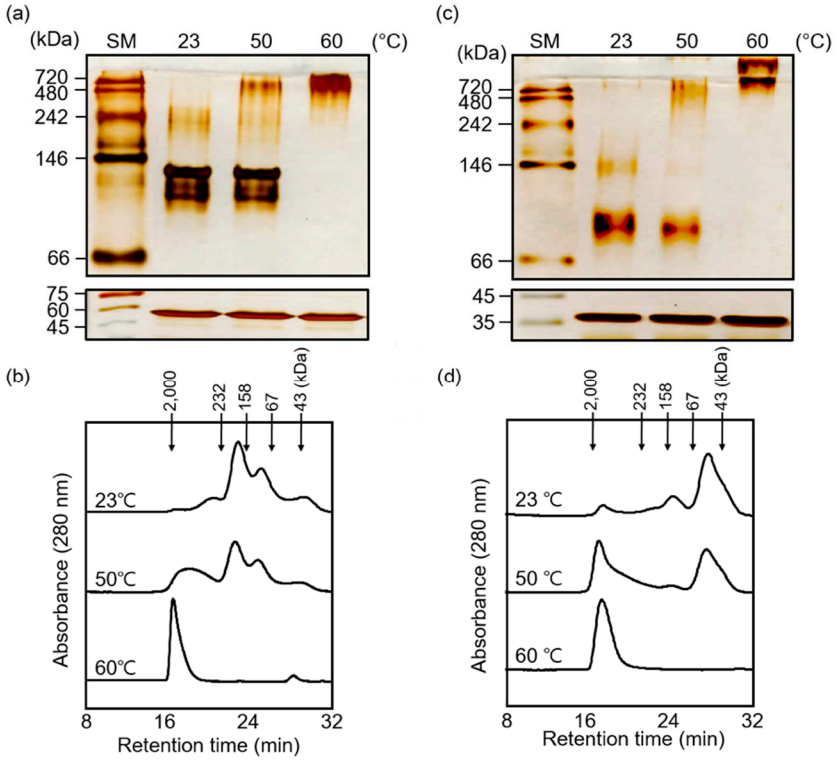

Figure 9. Heat shock-dependent structural changes in AtTPR10, ANK-D, and TPR-D. (**a**)–(**d**) Analysis of heat shock-dependent structural changes by 10% native gel electrophoresis (**a**) and (**c**) and SEC using HPLC (**b**) and (**d**) upon incubation at different temperatures (23 °C, 50 °C, and 60 °C) for 30 min. SM represents the size marker (**a**) and (**c**).

Overall, our results demonstrate that AtTPR10 acts as a molecular chaperone to protect plants from heat stress, and the ANK and TPR domains of AtTPR10 work together to enhance its chaperone function. Given that *Arabidopsis* contains a number of AtTPR isotypes (Figure 1), it is possible that most of these proteins perform the same basic function as AtTPR10, in addition to other specific roles in the regulation of diverse plant processes.

4. Discussion

Because plants are sessile organisms, protection from temperature fluctuations is critical for their survival. Thus, plants have developed a number of tools or systems to combat environmental stresses. Among these, molecular chaperone proteins that support the structural assembly or disassembly of intracellular target substrates and maintain their conformational folding contribute to the protection of plants from diverse external stresses. Most of the HSPs, including HSP60, HSP70, HSP90, and small HSPs, are distributed in all living organisms, ranging from bacteria to humans, and function as chaperones. The expression of genes encoding these HSPs is induced by diverse environmental factors, including cold, chemical treatment, wounding, and ultraviolet (UV) light. HSPs not only stabilize newly synthesized proteins to ensure correct folding but also repair misfolded proteins damaged by internal or external stresses. As the name implies, HSPs primarily function under heat shock by stabilizing heat stress-denatured molten-globular target substrates and renaturing these proteins to form native structures after the stresses are removed [28,29]. To mediate interaction between the partially denatured and unstructured proteins/peptides and to prevent the self-aggregation of substrates, chaperone proteins contain hydrophobic surfaces. The TPR and ANK domains are highly optimized to perform this function since they have an irregular structure with a large proportion of hydrophobic residues. Based on these structural characteristics, the TPR domain is reported to function as a co-chaperone in association with HSP90/70 [37–39]. Other *Arabidopsis* proteins such as protein phosphatase 5 (PP5) [34] and the Trx domain-containing protein AtTDX, which functions as a disulfide reductase [21], also contain TPR domains. In these proteins, TPR domains are involved in protein–protein interactions, protein assembly, and signal transduction. Overexpression of genes encoding TPR domain-containing proteins has been shown to enhance heat shock tolerance in plants [40,41].

Similarly, the ANK domain first discovered in the yeast Cdc10 protein contains 4–6 repeats of a 33 aa motif, forming two α-helices and a separate type 1 β-bulge loop [14,42]. The lateral surface structure of these repeats is hydrophobic with changeable conformation, which is mainly responsible for protein–protein interactions. The ANK domain forms a linear solenoid structure and performs multiple functions, including cell cycle control, ion transport, and signal transduction via protein–protein interactions. The ANK domain is present in several important proteins including the non-expressor of PR1 (NPR1), which functions as a key regulator of systemic acquired resistance (SAR) [43,44]; accelerated cell death 6 protein (ACD6), which contains one ANK motif and regulates plant defense via salicylic acid signaling [45]; and the nuclear-located ANK protein in tobacco, which enhances the auxin-mediated bZIP transcription factors, BZI-1 and BZI-2, through its regulation of protein complex formation [46]. These proteins also participate in pathogen resistance and hormone signaling [44–46]. In addition, the ANK repeat-containing protein 2A (AKR2A) protects its targets from stress-induced aggregation. In *Arabidopsis*, APX3 and the outer envelope protein 7 (OEP7) work together in chloroplasts to maintain plant growth and development [47]. In humans, mutation of *ANK* genes has a critical effect on the association of the encoded protein with the cell cycle inhibitor p16 or Notch protein, resulting in diverse diseases such as cancer, neurological disorders including alcoholism, nicotine dependency, obesity, and juvenile delinquency [14,48,49]. Thus, investigation of ANKs and TPRs is highly important to understand the regulation of their protein–protein interaction activity, identify the crucial residues needed for signal transduction, and control their chaperone function in plants. Understanding the regulation of *AtTPR10* expression and chaperone function in future studies will enable the development of stress-tolerant crops.

Author Contributions: Conceptualization, S.K.P., C.H.K., Y.H.C., and S.Y.L.; methodology, S.K.P., H.B.C., and C.H.K.; validation, E.S.L. and J.H.P.; formal analysis, S.K.P., Y.H.C., and S.Y.L.; investigation, S.K.P.; resources, S.D.W., S.B.B., and K.A.T.P.; draft writing, review, and editing, S.K.P. and S.Y.L.; funding acquisition, H.B.C. and S.Y.L. All authors have read and agreed to the published version of the manuscript.

Funding: This research was funded by the NG-BioGreen21 program (SSAC, PJ013173), RDA, Korea (S.Y.L.), and the Basic Science Research Program through the National Research Foundation (NRF) of Korea funded by the ministry of Education (Grant No. 2018R1A6A3A11049525 to H.B.C.).

Conflicts of Interest: The authors declare no conflict of interest.

References

1. Blatch, G.L.; Lässle, M. The tetratricopeptide repeat: A structural motif mediating protein-protein interactions. *BioEssays* **1999**, *21*, 932–939. [CrossRef]
2. Zeytuni, N.; Zarivach, R. Structural and Functional Discussion of the Tetra-Trico-Peptide Repeat, a Protein Interaction Module. *Structure* **2012**, *20*, 397–405. [CrossRef] [PubMed]
3. Cerveny, L.; Straskova, A.; Dankova, V.; Hartlova, A.; Ceckova, M.; Staud, F.; Stulik, J. Tetratricopeptide Repeat Motifs in the World of Bacterial Pathogens: Role in Virulence Mechanisms. *Infect. Immun.* **2013**, *81*, 629–635. [CrossRef] [PubMed]
4. Bose, S.; Weikl, T.; Bügl, H.; Buchner, J. Chaperone Function of Hsp90-Associated Proteins. *Science* **1996**, *274*, 1715–1717. [CrossRef]
5. Mok, D.; Allan, R.K.; Carrello, A.; Wangoo, K.; Walkinshaw, M.D.; Ratajczak, T. The chaperone function of cyclophilin 40 maps to a cleft between the prolyl isomerase and tetratricopeptide repeat domains. *FEBS Lett.* **2006**, *580*, 2761–2768. [CrossRef]
6. Yan, J.; Wang, J.; Li, Q.; Hwang, J.R.; Patterson, C.; Zhang, H. AtCHIP, a U-Box-Containing E3 Ubiquitin Ligase, Plays a Critical Role in Temperature Stress Tolerance in Arabidopsis1. *Plant Physiol.* **2003**, *132*, 861–869. [CrossRef]
7. Rosser, M.F.N.; Washburn, E.; Muchowski, P.J.; Patterson, C.; Cyr, U.M. Chaperone Functions of the E3 Ubiquitin Ligase CHIP. *J. Boil. Chem.* **2007**, *282*, 22267–22277. [CrossRef]
8. Schapire, A.L.; Valpuesta, V.; Botella, M.A. TPR Proteins in Plant Hormone Signaling. *Plant Signal. Behav.* **2006**, *1*, 229–230. [CrossRef]
9. Rosado, A.; Schapire, A.L.; Bressan, R.A.; Harfouche, A.L.; Hasegawa, P.M.; Valpuesta, V.; Botella, M. Ángel The Arabidopsis Tetratricopeptide Repeat-Containing Protein TTL1 Is Required for Osmotic Stress Responses and Abscisic Acid Sensitivity1. *Plant Physiol.* **2006**, *142*, 1113–1126. [CrossRef]
10. Tseng, T.-S. Ectopic Expression of the Tetratricopeptide Repeat Domain of SPINDLY Causes Defects in Gibberellin Response. *Plant Physiol.* **2001**, *126*, 1250–1258. [CrossRef]
11. Park, S.-C.; Kim, I.R.; Hwang, J.E.; Kim, J.-Y.; Jung, Y.J.; Choi, W.; Lee, Y.; Jang, M.-K.; Lee, J.R. Functional Mechanisms Underlying the Antimicrobial Activity of the Oryza sativa Trx-like Protein. *Int. J. Mol. Sci.* **2019**, *20*, 1413. [CrossRef] [PubMed]
12. Yang, C.; Yu, Y.; Huang, J.; Meng, F.; Pang, J.; Zhao, Q.; Islam, A.; Xu, N.; Tian, Y.; Liu, J.; et al. Binding of the Magnaporthe oryzae Chitinase MoChia1 by a Rice Tetratricopeptide Repeat Protein Allows Free Chitin to Trigger Immune Responses. *Plant Cell* **2019**, *31*, 172–188. [CrossRef] [PubMed]
13. Sedgwick, S.G.; Smerdon, S.J. The ankyrin repeat: A diversity of interactions on a common structural framework. *Trends Biochem. Sci.* **1999**, *24*, 311–316. [CrossRef]
14. Mosavi, L.K.; Cammett, T.J.; Desrosiers, D.C.; Peng, Z.-Y. The ankyrin repeat as molecular architecture for protein recognition. *Protein Sci.* **2004**, *13*, 1435–1448. [CrossRef] [PubMed]
15. Michaely, P.; Bennett, V. The ANK repeat: A ubiquitous motif involved in macromolecular recognition. *Trends Cell Boil.* **1992**, *2*, 127–129. [CrossRef]
16. Rohde, K.; Bork, P. A fast, sensitive pattern-matching approach for protein sequences. *Bioinformatics* **1993**, *9*, 183–189. [CrossRef]
17. Bork, P. Hundreds of ankyrin-like repeats in functionally diverse proteins: Mobile modules that cross phyla horizontally? *Proteins Struct. Funct. Genet.* **1993**, *17*, 363–374. [CrossRef]
18. Miranda-Vizuete, A.; Damdimopoulos, A.E.; Gustafsson, J.-Å.; Spyrou, G. Cloning, expression, and characterization of a novel Escherichia coli thioredoxin. *J. Boil. Chem.* **1997**, *272*, 30841–30847. [CrossRef]
19. Collet, J.-F.; Jakob, U.; Bardwell, J.C.A.; D'Souza, J.C. Thioredoxin 2, an Oxidative Stress-induced Protein, Contains a High Affinity Zinc Binding Site. *J. Boil. Chem.* **2003**, *278*, 45325–45332. [CrossRef]

20. Lohmann, C.; Eggers-Schumacher, G.; Wunderlich, M.; Schoffl, F. Two different heat shock transcription factors regulate immediate early expression of stress genes in Arabidopsis. *Mol. Genet. Genom.* **2004**, *271*, 376. [CrossRef]
21. Lee, J.R.; Lee, S.S.; Jang, H.H.; Lee, Y.M.; Park, J.H.; Park, S.-C.; Moon, J.C.; Park, S.K.; Kim, S.Y.; Lee, S.Y.; et al. Heat-shock dependent oligomeric status alters the function of a plant-specific thioredoxin-like protein, AtTDX. *Proc. Natl. Acad. Sci. USA* **2009**, *106*, 5978–5983. [CrossRef] [PubMed]
22. Sharma, K.K.; Kaur, H.; Kumar, G.S.; Kester, K. Interaction of 1,1′-Bi(4-anilino)naphthalene-5,5′-Disulfonic Acid with a-Crystallin. *J. Biol. Chem.* **1998**, *273*, 8965–8970. [CrossRef] [PubMed]
23. Jang, H.H.; Lee, K.O.; Chi, Y.H.; Jung, B.G.; Park, S.K.; Park, J.H.; Lee, J.R.; Lee, S.S.; Moon, J.C.; Yun, J.W.; et al. Two enzymes in one; two yeast peroxiredoxins display oxidative stress-dependent switching from a peroxidase to a molecular chaperone function. *Cell* **2004**, *117*, 625–635. [CrossRef] [PubMed]
24. Charng, Y.; Liu, H.; Liu, N.; Chi, W.; Wang, C.; Chang, S.; Wang, T. A Heat-Inducible Transcription Factor, HsfA2, Is Required for Extension of Acquired Thermotolerance in Arabidopsis. *Plant Physiol.* **2007**, *143*, 251–262. [CrossRef] [PubMed]
25. Xu, Z.-Y.; Zhang, X.; Schläppi, M.; Xu, Z.-Q. Cold-inducible expression of AZI1 and its function in improvement of freezing tolerance of Arabidopsis thaliana and Saccharomyces cerevisiae. *J. Plant Physiol.* **2011**, *168*, 1576–1587. [CrossRef] [PubMed]
26. Taji, T.; Seki, M.; Satou, M.; Sakurai, T.; Kobayashi, M.; Ishiyama, K.; Narusaka, Y.; Narusaka, M.; Zhu, J.-K.; Shinozaki, K. Comparative Genomics in Salt Tolerance between Arabidopsis and Arabidopsis-Related Halophyte Salt Cress Using Arabidopsis Microarray1. *Plant Physiol.* **2004**, *135*, 1697–1709. [CrossRef]
27. Cha, J.-Y.; Kim, W.-Y.; Bin Kang, S.; Kim, J.I.; Baek, N.; Jung, I.J.; Kim, M.R.; Li, N.; Kim, H.-J.; Nakajima, M.; et al. A novel thiol-reductase activity of Arabidopsis YUC6 confers drought tolerance independently of auxin biosynthesis. *Nat. Commun.* **2015**, *6*, 8041. [CrossRef]
28. Yao, J.; Sun, D.; Cen, H.; Xu, H.; Weng, H.; Yuan, F.; He, Y. Phenotyping of Arabidopsis Drought Stress Response Using Kinetic Chlorophyll Fluorescence and Multicolor Fluorescence Imaging. *Front. Plant Sci.* **2018**, *9*, 603. [CrossRef]
29. Moon, J.C.; Hah, Y.-S.; Kim, W.Y.; Jung, B.G.; Jang, H.H.; Lee, J.R.; Kim, S.Y.; Lee, Y.M.; Jeon, M.G.; Kim, C.W.; et al. Oxidative Stress-dependent Structural and Functional Switching of a Human 2-Cys Peroxiredoxin Isotype II That Enhances HeLa Cell Resistance to H2O2-induced Cell Death. *J. Boil. Chem.* **2005**, *280*, 28775–28784. [CrossRef]
30. Scheufler, C.; Brinker, A.; Bourenkov, G.; Pegoraro, S.; Moroder, L.; Bartunik, H.; Hartl, F.U.; Moarefi, I. Structure of TPR Domain–Peptide Complexes: Critical Elements in the Assembly of the Hsp70–Hsp90 Multichaperone Machine. *Cell* **2000**, *101*, 199–210. [CrossRef]
31. Das, A.K.; Cohen, P.W.; Barford, D. The structure of the tetratricopeptide repeats of protein phosphatase 5: Implications for TPR-mediated protein-protein interactions. *EMBO J.* **1998**, *17*, 1192–1199. [CrossRef] [PubMed]
32. Becerra, C.; Jahrmann, T.; Puigdomènech, P.; Vicient, C.M. Ankyrin repeat-containing proteins in Arabidopsis: Characterization of a novel and abundant group of genes coding ankyrin-transmembrane proteins. *Gene* **2004**, *340*, 111–121. [CrossRef] [PubMed]
33. Yan, J.; Wang, J.; Zhang, H. An ankyrin repeat-containing protein plays a role in both disease resistance and antioxidation metabolism. *Plant J.* **2002**, *29*, 193–202. [CrossRef] [PubMed]
34. Park, J.H.; Lee, S.Y.; Kim, W.Y.; Jung, Y.J.; Chae, H.B.; Jung, H.S.; Kang, C.H.; Shin, M.R.; Kim, S.Y.; Su'Udi, M.; et al. Heat-induced chaperone activity of serine/threonine protein phosphatase 5 enhances thermotolerance in Arabidopsis thaliana. *New Phytol.* **2011**, *191*, 692–705. [CrossRef]
35. Kang, C.H.; Lee, S.Y.; Park, J.H.; Lee, Y.; Jung, H.S.; Chi, Y.H.; Jung, Y.J.; Chae, H.B.; Shin, M.R.; Kim, W.Y.; et al. Stress-driven structural and functional switching of Ypt1p from a GTPase to a molecular chaperone mediates thermo tolerance in Saccharomyces cerevisiae. *FASEB J.* **2015**, *29*, 4424–4434. [CrossRef]
36. Lee, E.M.; Lee, S.S.; Tripathi, B.N.; Jung, H.S.; Cao, G.P.; Lee, Y.; Singh, S.; Hong, S.H.; Lee, K.W.; Lee, S.Y.; et al. Site-directed mutagenesis substituting cysteine for serine in 2-Cys peroxiredoxin (2-Cys Prx A) of Arabidopsis thaliana effectively improves its peroxidase and chaperone functions. *Ann. Bot.* **2015**, *116*, 713–725. [CrossRef]
37. Mayer, M.P.; Gierasch, L.M. Recent advances in the structural and mechanistic aspects of Hsp70 molecular chaperones. *J. Biol. Chem.* **2019**, *294*, 2085–2097. [CrossRef]

38. Rosenzweig, R.; Nillegoda, N.B.; Mayer, M.P.; Bukau, B. The Hsp70 chaperone network. *Nat. Rev. Mol. Cell Boil.* **2019**, *20*, 665–680. [CrossRef]
39. Vo, K.T.X.; Kim, C.-Y.; Chandran, A.K.N.; Jung, K.-H.; An, G.; Jeon, J.-S. Molecular insights into the function of ankyrin proteins in plants. *J. Plant Boil.* **2015**, *58*, 271–284. [CrossRef]
40. Park, S.K.; Jung, Y.J.; Lee, J.R.; Lee, Y.M.; Jang, H.H.; Lee, S.S.; Park, J.H.; Kim, S.Y.; Moon, J.C.; Lee, S.Y.; et al. Heat-Shock and Redox-Dependent Functional Switching of an h-Type Arabidopsis Thioredoxin from a Disulfide Reductase to a Molecular Chaperone1. *Plant Physiol.* **2009**, *150*, 552–561. [CrossRef]
41. Chae, H.B.; Moon, J.C.; Shin, M.R.; Chi, Y.H.; Jung, Y.J.; Lee, S.Y.; Nawkar, G.M.; Jung, H.S.; Hyun, J.K.; Kim, W.Y.; et al. Thioredoxin Reductase Type C (NTRC) Orchestrates Enhanced Thermotolerance to Arabidopsis by Its Redox-Dependent Holdase Chaperone Function. *Mol. Plant* **2013**, *6*, 323–336. [CrossRef]
42. Tamura, K.; Taniguchi, Y.; minoguchi, S.; Sakai, T.; Tun, T.; Furukawa, T.; Honjo, T. Physical interaction between a novel domain of the receptor Notch and the transcription factor RBP-Jκ/Su(H). *Curr. Boil.* **1995**, *5*, 1416–1423. [CrossRef]
43. Cao, H.; Glazebrook, J.; Clarke, J.D.; Volko, S.; Dong, X. The Arabidopsis NPR1 Gene That Controls Systemic Acquired Resistance Encodes a Novel Protein Containing Ankyrin Repeats. *Cell* **1997**, *88*, 57–63. [CrossRef]
44. Kinkema, M.; Fan, W.; Dong, X. Nuclear Localization of NPR1 Is Required for Activation of PR Gene Expression. *Plant Cell* **2000**, *12*, 2339–2350. [CrossRef] [PubMed]
45. Lu, H.; Rate, D.N.; Song, J.T.; Greenberg, J.T. ACD6, a Novel Ankyrin Protein, Is a Regulator and an Effector of Salicylic Acid Signaling in the Arabidopsis Defense Response. *Plant Cell* **2003**, *15*, 2408–2420. [CrossRef]
46. Böttner, S.; Iven, T.; Carsjens, C.S.; Dröge-Laser, W. Nuclear accumulation of the ankyrin repeat protein ANK1 enhances the auxin-mediated transcription accomplished by the bZIP transcription factors BZI-1 and BZI-2. *Plant J.* **2009**, *58*, 914–926. [CrossRef]
47. Shen, G.; Kuppu, S.; Venkataramani, S.; Wang, J.; Yan, J.; Qiu, X.; Zhang, H. ANKYRIN REPEAT-CONTAINING PROTEIN 2A is an essential molecular chaperone for peroxisomal membrane-bound ASCORBATE PEROXIDASE3 in Arabidopsis. *Plant Cell* **2010**, *22*, 811–831. [CrossRef]
48. Kang, Y.; Xie, H.; Zhao, C. Ankrd45 Is a Novel Ankyrin Repeat Protein Required for Cell Proliferation. *Genes* **2019**, *10*, 462. [CrossRef]
49. Neville, M.J.; Johnstone, E.C.; Walton, R.T. Identification and characterization of ANKK1: A novel kinase gene closely linked to DRD2 on chromosome band 11q23.1. *Hum. Mutat.* **2004**, *23*, 540–545. [CrossRef]